A new Denoising Filter for Brain MR Images

Ashish Phophalia*
DAIICT
Gujrat, India
ce.pashish@gmail.com

Suman K. Mitra
DAIICT
Gujrat, India
suman_mitra@daiict.ac.in

Ajit Rajwade
DAIICT
Gujrat, India
ajit_rajwde@daiict.ac.in

ABSTRACT

A new denoising filter is proposed for human brain MR image. The proposed filter is based on the notion of existing bilateral filter whose objective is to get a noise-free smooth image, preserving edges and other features intact. We have introduced a weighing function that controls the impact of existing bilateral filter for denoising. It is conditioned by Rough Edge Map (REM) and Rough Class Label (RCL). The presence of noise makes difficult to get precise information of edge and class label. Rough Set Technique is expected to assign rough (imprecise) class label and edge label to the pixels in the given image. This function thus is expected to handle the impreciseness of edge and class label and thereby preserving these two by controlling the bilateral filter more efficiently. The filter is extensively applied on brain MR images. The current proposal is compared with some of state-of-the-art approaches using different image quality measures and found to be efficient in most of the cases.

Keywords

Image Denoising, Magnetic Resonance Imaging (MRI), Rough Set Theory

1. INTRODUCTION

Image denoising is a preprocessing step that makes subsequent image analysis procedure easier. The objective of this step is to lower down noise component from the noisy image while preserving its important features like edges, corner points etc. Usually, noise model is assumed as

$$Y_{i,j} = X_{i,j} + \eta_{i,j} \tag{1}$$

where η the noise attached to the $(i,j)^{th}$ pixel of the image X. The denoising approach estimates X which is as noiseless as possible from the given noisy image Y.

*Corresponding author

ICVGIP '12, December 16-19, 2012, Mumbai, India

Several attempts have been made towards estimating noiseless image without assuming any noise distribution. Mostly, a filter is designed which when applied to the noisy image Y is expected to eliminate the noise and give rise to an estimate of X. The Mean and Median filters are very primitive towards this goal. More sophisticated filter called isotropic diffusion based on Gaussian kernel was an improvement towards this task. This, when extended to Anisotropic diffusion [13], [18], sets the goal high for the researchers. Further development has been made by incorporating robust statistics [3], probability based approach [1] and adaptive smoothing edge map [14].

Furthermore, non-iterative and more edge preserving Bilateral filters [16] are designed for denoising. It uses two filters, one on spatial location and another on intensity values, simultaneously. Since its inception, there has been many modifications of bilateral filter suggested [2], [8]. It is even extended to Trilateral filters. The third filter which is used simultaneously with bilateral is designed in various ways [19], [5]. It could be concluded that more informative the filters are better is the result expected. With this aim in mind, we are proposing a new denoising filter for Brain MR Imaging. The new set of filters includes the information regarding spatial variation and intensity variation that are conditioned on edge map and class label within a neighborhood. Each image pixel is classified as an edge or non-edge pixel (edge map) and its belongingness to an object (class label) within the image. A Rough set based approach has been explored to obtain an Edge Map and Class label. Note that the basic structure of bilateral filters remains same.

The main intention of the current work is to suggest a noise removal approach for the set of images where object boundaries are imprecise in nature. In medical images such as Brain MR images, the object boundaries are not only imprecise but also confusing due to the noise generated by machine sensors, patient movements, technician expertise etc. Most of the denoising approaches for the medical images assume the noise to be Gaussian however attempts have been made where same is modeled by Rician [11]. The proposed filter is independent of assumption on noise distribution present in the image. To capture object boundaries from the notion of impreciseness, Rough Set Theory (RST) [12] is utilized. RST is a popular mathematical tool that deals with imprecise information. Note that the RST has already been utilized in Medical image analysis [6].

In this work, keeping the structure of bilateral filter as it is, we intended to make it more informative. A Rough set based Edge Map (REM) and Class label (RCL) are used

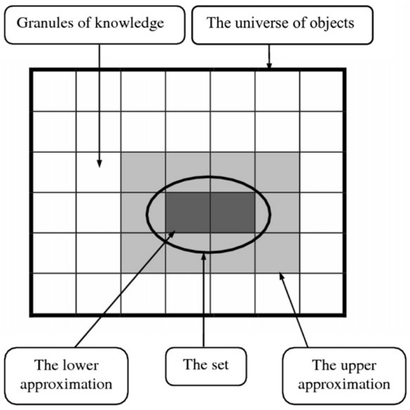

Figure 1: Concept of estimating the object boundaries in Rough Set [12]

along with spatial and intensity information. The information regarding REM strongly controls the effect of bilateral filter on edge and non-edge pixel whereas the RCL keeps track of the homogeneity within object and heterogeneity on the edges. The performance of the proposed method is tested on a large set of Brain MR images and the results are compared with many existing techniques. The four different quantitative measures such as Peak Signal to Noise Ration (PSNR), Root Mean Squared Error (RMSE) and Mean Structure Similarity (M-SSIM) measure [17] and Feature Similarity (FSIM) measure [20] are used for comparing the performance of the denoising techniques. Note that, more or less these quantitative measures are used by the researchers.

The paper is organized in following way: Section 2 presents the proposed approach for MR image denoising problem, Section 3 presents experimental results on human brain MR images with visual examples and comparison with some of the state-of-the-art algorithms. Section 4 concludes the manuscript.

2. PROPOSED APPROACH

The object boundaries in monochrome images is often ill-defined because of grayness or spatial ambiguity [10]. This notion leads to use Rough set based edge information instead standard edge detectors used in image processing literature. Using granule based processing, objects can be partitioned into their lower and upper approximations. One simple example of lower and upper approximation of object in an image is shown in Figure 1.

Information such as class label and edge map are derived from the lower and upper approximations for each object present in the image. So far Rough Set, in other words lower and upper approximations, has been successfully used for binarization of any image assuming that the image contains only one object [10], [9]. However, Brain MR image which is current interest, contains at least 3 classes. So the concept of Rough Set binarization is extended towards multi class problem. Note that multiple thresholding problem using rough entropy criteria has been addressed in [7] that uses genetic algorithm. We are presenting here, a simple histogram based approach. The next subsection explains derivation of class information from multiple thresholding.

2.1 Derivation of Class Information

Our goal is to assign a class label to each pixel of the image. Though, there are many ways to do it, however impreciseness present in the image due to noise plays a major role. We are not intended to assign class label in precise way and hence Rough set is used. The histogram of brain MR image is expected to be multi model due the presence of more than one class. The concept of Rough Set based binarization (two class problem) is utilized successively considering one of the objects as the object of interest and the remaining objects including background as background. Successive use of binarization will be leading towards multiple optimized thresholding of histogram. Figure 2 is showing histogram of a synthetically generated image that contains two objects in a background and two thresholds, namely T_1 and T_2 along with the regions less than or greater than the thresholds.

As an initial step, approximate thresholds (valleys in the histogram) are obtained. A window based approach is adopted to find local minima or valleys or thresholds from the histogram. The window size could be varied to get desired number of thresholds from brain MR image. In the next step, the approximate thresholds are optimized separately using Rough Entropy measure. The optimization of rough entropy reveals minimizing roughness of the object at a threshold T. In this work, the rough entropy function used is defined in [15], which is as follows

$$RE_T = -\frac{1}{2}\left[R_{O_T} log_e\left(\frac{R_{O_T}}{e}\right) + R_{B_T} log_e\left(\frac{R_{B_T}}{e}\right)\right] \quad (2)$$

where $R_{O_T} = 1 - |\overline{O}_T| \,/\, |\underline{O}_T|$ and $R_{B_T} = 1 - |\overline{B}_T| \,/\, |\underline{B}_T|$ ($|\overline{A}|$ and $|\underline{A}|$ are cardinalities of lower and upper approximation of set A respectively) are roughness of object and background respectively.

The image under consideration is binarized for each threshold and a pixel is given a symbol either 0 or 1 for each threshold. Thus, a pixel will get K such symbols for K thresholds present in the image. Each pixel could then be represented by a binary string of length K. On classifying the binary string with respect to the symbols and their positions, we can assign a class label for each pixel. A figurative explanation is shown in Figure 3.

The entire procedure is summarized below:

- Estimate approximate thresholds from the noisy image histogram using parzen window approach.
- Optimize each threshold separately using rough entropy criteria (Eq. 2).

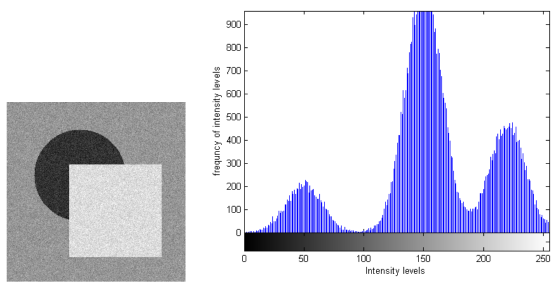

(a) (b)

Figure 2: Noisy image and its Histogram

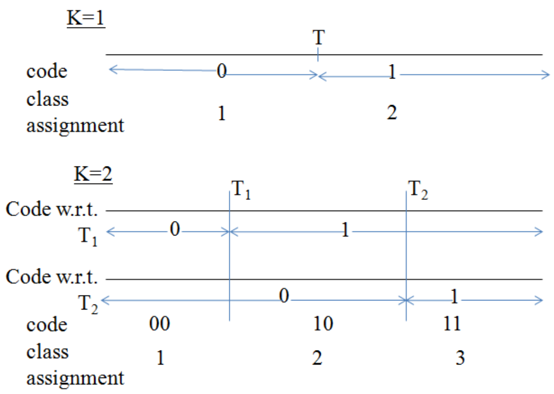

Figure 3: Code and Class assignment for different number of thresholds. Here K is number of thresholds.

- Binarize the image with respect to each optimized threshold. For each threshold, assign 1 if pixel value is greater or equal to the threshold, 0 otherwise.
- Combine assigned symbols (1 or 0) of each pixel for all thresholds. This will lead to representing each pixel by a binary string of length K, if there are K thresholds.
- Classify all binary strings and there by pixels. Strings having same symbol at same position will be classified as same class.

The above procedure is implemented on synthetically generated image which has two objects and a background. The stepwise results are shown in Figure 4. The threshold of this synthetic image is already shown in Figure 2.

2.2 Derivation of Rough Edge Map (REM)

While deriving the class information through optimized threshold (as described in subsection 2.1) by optimizing rough entropy (Eq 2), it has been observed that rough entropy is optimized if for each object, cardinality of object upper(O_U) and object lower (O_L) are same. In other words, these could be looked upon as a very precise and thin edge existing in between object and background. This ideal situation can not be obtained in case of digitized image and that to if noisy. To obtain the cardinality of lower and upper approximation of the object, a granule based method is adopted. The minimum granule size could be 1×2, 2×1 or 2×2. This leads to a situation where some granules will not be counted entirely in lower approximation or entirely in upper approximation. These granules, thus could be considered as thick rough edge of the object.

The above notion is utilized to derive Rough Edge Map (REM). Each optimized threshold (as described in subsection 2.1) will generate a thick (e.g. 2×2 blocks) rough edge map for the object under consideration. Corresponding to each threshold and thereby corresponding to each object, we get separate rough edge map of each object. Now, the union of all such rough edge maps is expected to fetch the rough edge map of the entire image. There could be commonality in rough edge maps of objects which are overlapping in the image. Such situation is easily handled by taking union of rough edge maps of the objects.

The whole problem thus boils down to finding set of granules that are not entirely included in lower or upper approximation of the object, when the image is binarized for that object. For each binarized image, we considered a granule of size 2×2. For each granule, find whether all the pixels in that are either 0 (object) or 1 (background). The granule containing pixel of type both 0 and 1, is called as mixed granule, and is included in the set of granules forming rough edge map. The process is repeated for each threshold. Finally, taking the union of such granules we get a rough edge map of the image. The results of this step on synthetically generated image is shown in Figure 5. Figure 6 shows the result of both the steps on MR image along with zoomed in part in Figure 7.

2.3 Proposed Denoising Filter

The conventional bilateral filter [16] defines weights as follows

$$\varphi(i,j) = \alpha(i,j)\beta(i,j) \tag{3}$$

where α and β are monotonically decreasing nonnegative functions respectively based on spatial closeness and intensity closeness between i and j. The α and β functions are mostly modeled as Gaussian function where the governing parameters σ_α and σ_β are application dependent based on neighborhood size. The denoised pixel is given by

$$\widehat{Y}_{i,j} = \frac{\sum_{j \in N(i)} \varphi(i,j) Y(i,j)}{\sum_{j \in N(i)} \varphi(i,j)} \tag{4}$$

where $Y(i,j)$ is the noisy image and $N(x)$ denotes neighborhood of x.

The proposed filter adds a new weighing factor to the conventional bilateral filter having two existing weighing factors

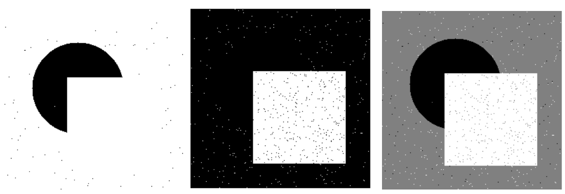

(a) (b) (c)

Figure 4: (a) Binary image corresponding to threshold T_1, (b) Binary image corresponding to threshold T_2 and (c) Class Information of the image shown in 2(a).

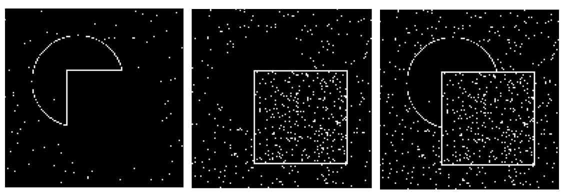

(a) (b) (c)

Figure 5: (a) Rough edges for first object corresponding to threshold T_1, (b)Rough edges for second object corresponding to threshold T_2, (c) Combining Rough Edge Map (REM) of the (a) and (b), the final REM is obtained.

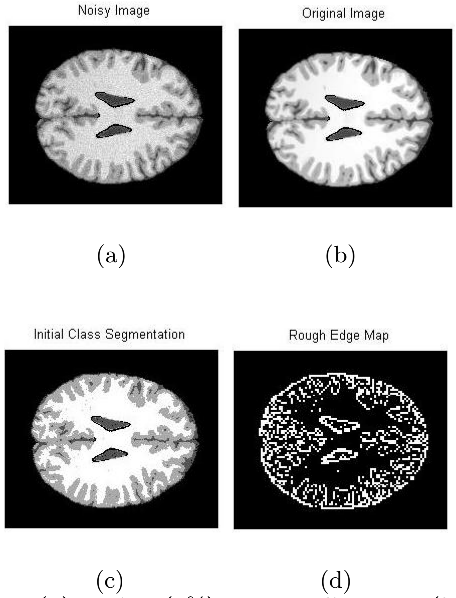

Figure 6: (a) Noisy (5%) Image slice 100, (b) Original Image Slice 100, (c) Initial Class labeled and (d) Rough Edge Map (granule size 2×2)

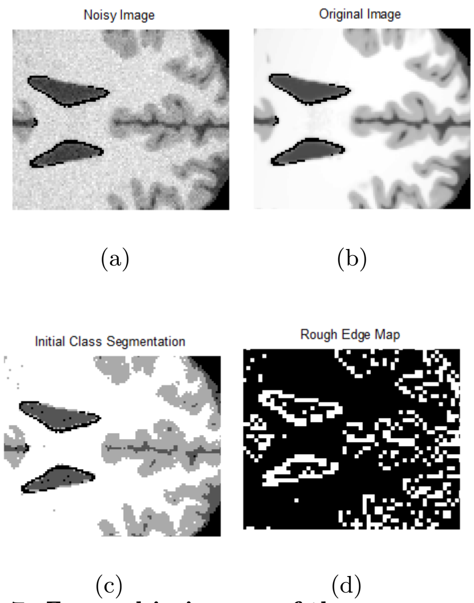

Figure 7: Zoomed in images of those represented in Fig.reff21 (a) Noisy (5%) Image slice 100, (b) Original Image Slice 100, (c) Initial Class labeled and (d) Rough Edge Map (granule size 2×2)

α and β (Eq. 3). The new weight assigned is spatial and adaptive in nature. The adaptiveness comes from the fact that it uses the neighborhood information of the pixel under consideration. Having three weighing function acting together, the proposed filter could be considered as *Trilateral filter* too. The value of third weight $\gamma(i,j) \in [0,1]$ is conditioned on Class information and REM as discussed in two previous subsections. Note that both class information and REM utilize the uncertainty or roughness of the image due to presence of noise. Hence, a fuzzy notion is introduced while deriving the value of γ depending on these two information. In this study, we used the three different notion of $\gamma(i,j)$, namely, small (γ_s), moderate (γ_m) and large (γ_l). We restrict the values of γ as follows:

1. $\gamma_s(i,j) \in [0, 0.4]$
2. $\gamma_m(i,j) \in (0.4, 0.7]$
3. $\gamma_l(i,j) \in (0.7, 1]$

So far, the ranges of small, medium and large values of γ are fixed intuitively by looking at its impact on the filter. However, a sigmoidal type of function could be used. The third weight (γ) is expected to either boost up or lower down the effect of other two weights in conventional bilateral filter. In fact, we introduced the notion of moderate impact of other two weights in the conventional bilateral filter by keeping moderate γ (γ_m). Basically, either γ_s, γ_m or γ_l is added to the conventional bilateral filter depending on the relationship of class information and rough edge map of the pixel under consideration with those of its neighbors. The neighbors of a pixel are defined by considering 3×3 window around it. The pseudo algorithm is as follows:

1. Construct a window of size 3×3 around the current pixel. let it be denoted by *Blk* centered at (x, y).
2. Normalize the pixels of *Blk* by maximum intensity present in *Blk*.
3. Define $Blk\_diff(i,j) = 1 - |Blk(i,j) - Blk(x,y)|$, $(i,j) \in Blk$. Here the absolute difference of the neighboring pixel from central pixel is subtracted from 1. This will make the center value 1 and other values accordingly.
4. Assign $\gamma(i,j)$ as follows:
   (a) if $REM(i,j) == 1$
   (b) if $class(i,j) == class(x,y)$
   (c) $\gamma(i,j) = \gamma_m$;
   (d) *else*
   (e) $\gamma(i,j) = \gamma_s$;
   (f) *end*
   (g) *else*
   (h) $if class(i,j) == class(x,y)$
   (i) $if REM(x,y) == 1$
   (j) $\gamma(i,j) = \gamma_m$;
   (k) *else*
   (l) $\gamma(i,j) = \gamma_l$;
   (m) *end*

(n) *else*

(o) $ifREM(x, y) == 1$

(p) $\gamma(i, j) = \gamma_s$;

(q) *else*

(r) $\gamma(i, j) = \gamma_s$; (This should not occur)

(s) *end*

(t) *end*

(u) *end*

The final filter designed is as follows:

$$\varphi(i, j) = \gamma(i, j)\alpha(i, j)\beta(i, j) \quad (5)$$

$$\alpha(i, j) = exp\left(-\frac{i^2 + j^2}{2\sigma_\alpha^2}\right)$$

$$\beta(i, j) = exp\left(-\frac{1}{2\sigma_\beta^2 Blk\_diff(i, j)}\right)$$

$$\gamma(i, j) = either\gamma_s, \gamma_m or \gamma_l$$

The final equation to estimate noiseless pixel remains same. The algorithm is based on following observations:

The first condition (a) emphasizes that whether neighbor pixel is near to an edge or not. The granule processing will give a thick edge which will also consider pixels near to actual edges. Conditions $(a) - (g)$ reveal that the edge may pass through neighbor pixel and both are from same class, so current pixel is also near to an edge hence assign moderate weight to preserve that edge. Otherwise both the pixel belong to different classes and hence assigned small weight.

If an edge is not passing through neighbor pixel then check whether they belong to same class or not in condition (h). If both are from same class and edge is passing from center pixel (condition (i)) then assign moderate weight to preserve that edge, otherwise (condition (k)), they both belong to homogeneous area and have high dependency on each other so assign large weight.

If both pixel and its neighbor do not belong to same class (condition (n)) and center pixel is an edge pixel (condition (o)) then both belong to different classes and edge is passing in between these two, so assign small weight. The condition (q) should not occur ideally (but this case has been observed in experiments), so assign small weight to have less impact on the current pixel.

3. EXPERIMENTAL RESULTS

The work has been carried out on $2D$ monochrome phantom human brain MR images. The volumetric data and ground truth data are downloaded from Brain Web database [4]. The experiments are performed on images having different noise levels. The specifications are as follows: Modality= T1, Protocol=ICBM, RF=20%. The presented work considered 4 classes in the image slice, namely Cerebrospinal Fluid (CSF), Gray Matter (GM), White Matter (WM) and Background. In this paper, we have compared 6 approaches, namely, (i) Median Filter, (ii) Mean Filter, (iii) Bilateral Filter [16], (iv) Trilateral filter with Impulse Detector (RTfilter) [5], (v) Scaled Bilateral Filter (ScaledBF) [2] and (vi) proposed approach. The result and analysis is not presented on real data set due to space limitation.

The first two approaches are the conventional **Median and Mean filters** where the center pixel of the window is replaced by either median value of the window or by mean value of that window respectively. The Median filter is one of the simplest way to eliminate impulse noise whereas Mean filter is for Gaussian kind of noise. The window size is the only application dependent parameter. Here, a 3×3 window is used for Mean and Median filters.

The **Bilateral filter** is applied on input noisy image after normalizing into range of $[0, 1]$. The parameters for it are $\sigma_\alpha = 1$ & $\sigma_\beta = 0.1$, adjusted experimentally. **Trilateral filter** with an Impulse detector [5] is implemented with parameter set kept as $\sigma_S = 1$, $\sigma_R = 16$, $\sigma_I = 50$ & $\sigma_P = 50$.

In case of **Scaled Bilateral Filter**, the selection of proper scale is a crucial task. Since lower scale will contain same noise amount whereas high scale may not preserve the details of Medical imaging where a single pixel conveys information. The scale is adjusted to 1 and two other parameters are kept same as Bilateral filter.

In the **proposed filter**, using the Class information and REM, the ranges of γ value can be defined based on application. Here, the γ values are kept as follows: $\gamma_s = 0.4$, $\gamma_m = 0.6$ & $\gamma_l = 0.9$. The granule size in computation of REM is of size 2×2. The number of parameters and their values used in are summarized in Table 1.

All approaches have been evaluated using four different quality measures. The Peak Signal to Noise Ratio (PSNR $= 10\log(\frac{255^2}{MSE(X,\widehat{X})})$) and Root Mean Square Error (RMSE) are simple in computation but do not consider human visual system. In image denoising problem, higher value of PSNR and lower values for RMSE are preferred.

$$RMSE = \frac{1}{MN}\left(\sum_{i=1}^{M}\sum_{j=1}^{N}\left(X(i, j) - \widehat{X}(i, j)\right)^2\right)^{1/2}$$

where the $X(i, j)$ is the ground truth intensity value, $\widehat{X}(i, j)$ is the estimated intensity value using noisy version of X and MSE is for mean squared error between X and $\widehat{X}$.

The Structure Similarity Index Measure (SSIM) [17] was proposed considering human vision system for comparing two images. The SSIM is window based measure which compare luminance, contrast and structure function of two windows of different images centered at same spatial location. The average of SSIM map can be considered as a single value to differentiate between two images, denoted as MSSIM.

$$SSIM(X, \widehat{X}) = \frac{4\sigma_{X\widehat{X}}\mu_X\mu_{\widehat{X}}}{\left(\sigma_X^2 + \sigma_{\widehat{X}}^2\right)\left(\mu_X^2 + \mu_{\widehat{X}}^2\right)}$$

Table 1: Number of Parameters and the values used in all the approaches

Approach	# of Parameters	Parameter value
Median filter	1	window size = 3
Mean filter	1	window size = 3
Bilateral filter	2	$\sigma_s = 1 \& \sigma_r = 0.1$
RTfilter	4	$\sigma_s = 1, \sigma_r = 16,$ $\sigma_I = 50 \& \sigma_P = 50$
ScaledBF	3	$\sigma_g = 1, \sigma_s = 1\&$ $\sigma_r = 0.1$
Proposed filter	3	$\sigma_s = 1, \sigma_r = 0.1\&\gamma$ $(\gamma_s = 0.4, \gamma_m = 0.6\&$ $\gamma_l = 0.9)$

$$MSSIM(X, \widehat{X}) = \frac{1}{M}\sum_{j=1}^{M} SSIM(X, \widehat{X})_j$$

where j is the total number of blocks in sliding window fashion. The MSSIM is computed on default window size i.e. 8×8 for all the experiments. Recently, another quality measure, Feature Similarity Index Measure (FSIM) [20],is proposed and is based on phase congruency and gradient magnitude of two images. The values of M-SSIM and FSIM are within $[0, 1]$ where 1 represents best case.

Table 2 includes comparison of all approaches on the basis of different quality measures. Bold values represent best values. The table shows experimental results for two slices having three different noise levels in volumetric data. By looking at the table in terms of PSNR and RMSE, it could be considered that the proposed filter performs better than other approaches. In terms of M-SSIM and FSIM, the proposed filter is either best or equivalent to one of the approach. Based on bilateral filter, this filter does not show very high difference with conventional approach but scale bilateral filter shows poor performance on medical images. Figure 8 shows the results of all approach and their zoomed in parts in Figure 9 for better visual comparison. The performance of scaled bilateral filter with others and proposed filter can be observed visually.

4. CONCLUSION

There are two main contributions of this paper. Initially a Rough Set based technique is developed to assign edge label (Yes/No) and class label to pixels present in the noisy MR image. These two informations are then efficiently utilized to propose a new weighing function, with the existing bilateral filters to control their impact while denoising the image, preserving edges. The introduction of this weighing function controls the impact of bilateral filters for preserving edges as its functionality is conditioned by the REM and RCL. The roughness or the impreciseness is obvious in the noisy environment and the current proposal effectively utilized that. The performance of the proposed denoting technique is quantitatively measured and compared with other contemporary techniques that use the concept of filters for denoising. The results obtained are found to be satisfactory both quantitatively and visually. It is mentioned earlier that the weighing function introduced has a fuzzy notion conditioned by REM and RCL. However the fuzzification has been done in a very simplistic manner as three specific values chosen experimentally to indicate small, moderate and large impact of this weighing function. Experiments are being carried out to automate these choices which would be adaptive in nature.

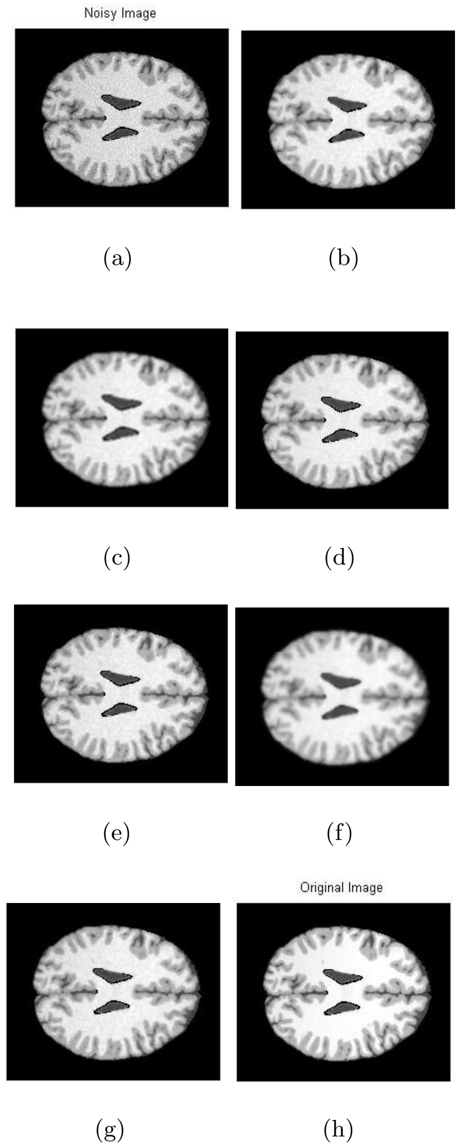

Figure 8: (a) Noisy Image, (b) Median filter (3×3), **(c) Mean filter** (3×3), **(d) Bilateral filter [16], (e) Trilateral filter [5], (f) Scaled Bilateral filter [2], (g) Proposed filter, (h) Original Image**

5. REFERENCES

[1] S. R. Arridge and A. Simmons. Multi-spectral probabilistic diffusion using bayesian classification. In *Scale space theory in computer vision*, pages 224–235, 1997.

[2] S. M. Aswatha, J. Mukhopadhyay, and P. Bhowmick. Image denoising by scaled bilateral filter. In *Third National Conference on Computer Vision, Pattern Recognition, Image Processing and Graphics*, pages 122–125, Dec. 2011.

[3] M. Black, G. Sapiro, D. H. Marimont, and D. Heeger. Robust anisotropic diffusion. *IEEE Trans. on Image Processing*, 7(3):421–432, March 1998.

Table 2: Performance comparison of proposed denoising filter with other approaches on various quantitative measures (The bold figure shows the best performance)

Images	Methods	PSNR (in dB)	RMSE	MSSIM	FSIM
Slice 70 (Noise 3%)	Noisy Image	33.82	26.96	0.96	0.967
	Median (3×3)	32.61	35.68	0.969	0.975
	Mean (3×3)	31.23	49.11	0.955	0.948
	Bilateral [16]	33.91	26.44	0.978	0.978
	RTfilter [5]	34.0	25.89	0.982	**0.982**
	ScaledBF [2]	29.07	80.61	0.896	0.9
	Proposed	**34.22**	**24.6**	**0.983**	**0.982**
Slice 100 (Noise 3%)	Noisy Image	33.75	27.39	0.96	0.961
	Median (3×3)	32.49	36.68	0.975	0.977
	Mean (3×3)	30.62	56.38	0.959	0.956
	Bilateral [16]	33.81	27.03	0.984	0.982
	RTfilter [5]	34.08	25.41	**0.986**	**0.984**
	ScaledBF [2]	28.72	87.22	0.914	0.919
	Proposed	**34.12**	**25.18**	**0.986**	**0.984**
Slice 70 (Noise 5%)	Noisy Image	29.45	73.21	0.91	0.932
	Median (3×3)	29.46	73.65	0.952	0.958
	Mean (3×3)	28.8	85.75	0.944	0.94
	Bilateral [16]	30.1	63.48	0.966	0.966
	RTfilter [5]	30.12	63.3	0.965	0.965
	ScaledBF [2]	27.45	116.83	0.889	0.896
	Proposed	**30.24**	**61.49**	**0.969**	**0.968**
Slice 100 (Noise 5%)	Noisy Image	29.44	74	0.914	0.918
	Median (3×3)	29.32	76.06	0.958	0.957
	Mean (3×3)	28.38	94.46	0.949	0.945
	Bilateral [16]	30	65.03	0.973	**0.969**
	RTfilter [5]	30.06	64.12	0.97	0.962
	ScaledBF [2]	27.13	125.25	0.908	0.914
	Proposed	**30.14**	**62.99**	**0.974**	0.967
Slice 70 (Noise 7%)	Noisy Image	29.02	81.44	0.856	0.891
	Median (3×3)	30.03	64.62	0.936	0.94
	Mean (3×3)	29.38	75.04	0.935	0.929
	Bilateral [16]	30.78	54.38	0.952	**0.952**
	RTfilter [5]	30.55	57.31	0.941	0.941
	ScaledBF [2]	27.92	104.97	0.887	0.893
	Proposed	**30.84**	**53.53**	**0.954**	0.95
Slice 100 (Noise 7%)	Noisy Image	29.06	80.74	0.867	0.879
	Median (3×3)	29.73	69.14	0.944	0.938
	Mean (3×3)	28.88	84.15	0.914	0.933
	Bilateral [16]	30.59	56.81	**0.96**	**0.952**
	RTfilter [5]	30.46	58.51	0.948	0.935
	ScaledBF [2]	27.58	113.65	0.907	0.912
	Proposed	**30.69**	**55.46**	**0.96**	0.946

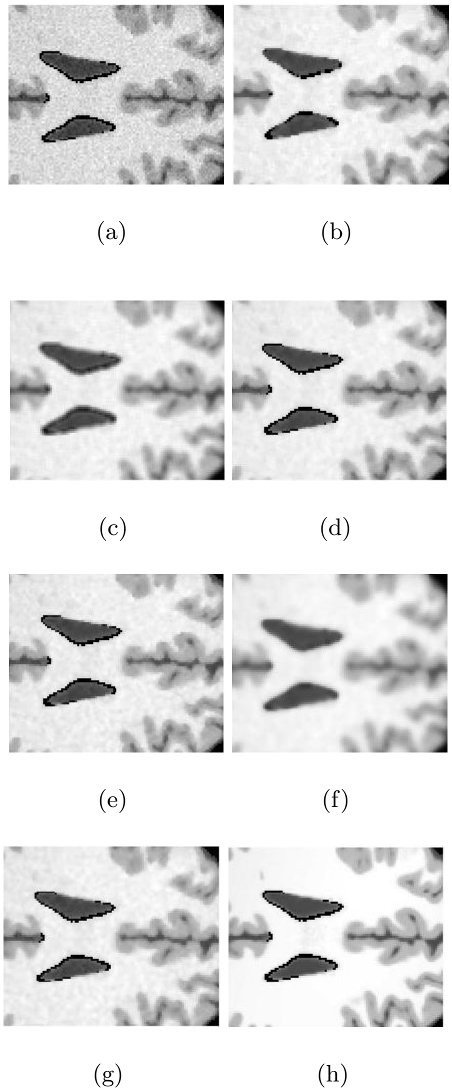

Figure 9: All images are zoomed in part of images showed in Fig. 8 (a) Noisy Image, (b) Median filter (3×3), (c) Mean filter (3×3), (d) Bilateral filter [16], (e) Trilateral filter [5], (f) Scaled Bilateral filter [2], (g) Proposed filter, (h) Original Image

[4] D. L. Collins, A. Zijdenbos, V. Kollokian, J. Sled, N. Kabani, C. Holmes, and A. Evans. Design and construction of a realistic digital brain phantom. *IEEE Trans. on Medical Imaging*, 17(3):463–468, June 1998.

[5] R. Garnett, T. Huegerich, C. Chui, and W. He. A universal noise removal algorithm with an impulse detector. *IEEE Trans. on Image Processing*, 14(11):1747–1754, November 2005.

[6] A. E. Hassanien, A. Abraham, J. F. Peters, G. Schaefer, and C. Henry. Rough sets and near sets in medical imaging: A review. *IEEE Trans. on Information Technology in Biomedicine*, 13(6):955–968, November 2009.

[7] D. Malyszko and J. Stepaniuk. Adaptive multilevel rough entropy evolutionary thresholding. *Information Sciences*, 180:1138–1158, 2010.

[8] S. K. Mitra and G. L. Sicuranza. *Nonlinear Image Processing*. Academic Press, 2000.

[9] P. Munshi and S. K. Mitra. A rough set based binarization technique for fingerprint images. In *IEEE International Conference on Signal Processing Computing and Control*, pages 1–6, March 2012.

[10] S. K. Pal, B. U. Shankar, and P. Mitra. Granular computing, rough entropy and object extraction. *Pattern Recognition Letters*, 26:2509–2517, 2005.

[11] S. Patz and H. Gudbjartsson. The rician distribution of noisy mri data. *Megn. Resonance Med.*, 34:910–914, 1995.

[12] Z. Pawlak and A. Skowron. Rudiments of rough sets. *Information Sciences*, 177:3–27, 2007.

[13] P. Perona and J. Malik. Scale space and edge detection using anisotropic diffusion. *IEEE Trans. on Pattern Ana. Mach. Intell.*, 12(7):629–639, July 1990.

[14] V. B. S. Prasath and A. Singh. Edge detectors based anisotropic diffusion for enhancement of digital images. In *Sixth Indian Conference on Computer Vision, Graphics and Image Processing*, pages 33–38, 2008.

[15] D. Sen and S. K. Pal. Histogram thresholding using beam theory and ambiguity measures. *Fundam. Inf.*, 75(1-4):483–504, 2007.

[16] C. Tomasi and R. Manduchi. Bilateral filtering for gray and color images. In *IEEE International Conference on Computer Vision*, pages 839–846, 1998.

[17] Z. Wang, A. C. Bovik, H. R. Sheikh, and E. P. Simoncelli. Image quality assessment: From error visibility to structural similarity. *IEEE Trans. on Image Processing*, 13(4):600–612, Apr. 2004.

[18] J. Weickart. *Anisotropic Diffusion in Image Processing*. B.G. Teubner Stuttgart, 1998.

[19] W. C. K. Wong, A. C. S. Chung, and S. C. H. Yu. Trilateral filtering for biomedical images. In *IEEE International Symposium on Biomedical Imaging: Nano to Macro*, pages 820–823, March 2004.

[20] L. Zhang, L. Zhang, X. Mou, and D. Zhang. Fsim: A feature similarity index for image quality assessment. *IEEE Trans. on Image Processing*, 20(9):2378–2386, Aug. 2011.